Qi et al. Stem Cell Research & Therapy (2024) 15:494
https://doi.org/10.1186/s13287-024-04114-3

Stem Cell Research & Therapy

RESEARCH Open Access

Near-infrared light induces neurogenesis and modulates anxiety-like behavior

Xing Qi[1,2†], Zhiliang Xu[3†], Xingchen Liu[1], Yanan Ren[1], Yecheng Jin[1], Wenjie Sun[1], Jiangxia Li[1], Duo Liu[4*], Shuwei Liu[2*], Qiji Liu[1,5*] and Xi Li[1*]

Abstract

Background The hippocampus is associated with mood disorders, and the activation of quiescent neurogenesis has been linked to anxiolytic effects. Near-infrared (NIR) light has shown potential to improve learning and memory in human and animal models. Despite the vast amount of information regarding the effect of visible light, there is a significant gap in our understanding regarding the response of neural stem cells (NSCs) to NIR stimulation, particularly in anxiety-like behavior. The present study aimed to develop a new optical manipulation approach to stimulate hippocampal neurogenesis and understand the mechanisms underlying its anxiolytic effects.

Methods We used 940 nm NIR (40 Hz) light exposure to stimulate hippocampal stem cells in C57BL/6 mice. The enhanced proliferation and astrocyte differentiation of NIR-treated NSCs were assessed using 5-ethynyl-2′-deoxyuridine (EdU) incorporation and immunofluorescence assays. Additionally, we evaluated calcium activity of NIR light-treated astrocytes using GCaMP6f recording through fluorescence fiber photometry. The effects of NIR illumination of the hippocampus on anxiety-like behaviors were evaluated using elevated plus maze and open-field test.

Results NIR light effectively promoted NSC proliferation and astrocyte differentiation via the OPN4 photoreceptor. Furthermore, NIR stimulation significantly enhanced neurogenesis and calcium-dependent astrocytic activity. Moreover, activating hippocampal astrocytes with 40-Hz NIR light substantially improved anxiety-like behaviors in mice.

Conclusions We found that flickering NIR (940 nm/40Hz) light illumination improved neurogenesis in the hippocampus with anxiolytic effects. This innovative approach holds promise as a novel preventive treatment for depression.

†Xing Qi and Zhiliang Xu contributed equally to this work.

*Correspondence:
Duo Liu
liuduo@sdu.edu.cn
Shuwei Liu
liusw@sdu.edu.cn
Qiji Liu
liuqiji@sdu.edu.cn
Xi Li
lixi@sdu.edu.cn

Full list of author information is available at the end of the article

Keywords Neural stem cells, NIR Light, Anxiety, Astrocytes, Calcium activity

Introduction

The hippocampus plays a crucial role in the pathophysiology of mood disorders, and alterations in its structure and function can impact adult neurogenesis [1, 2]. The activation of granule cells in the dentate gyrus (DG) of the hippocampus induces anxiolytic effects [3, 4]. NSCs within the subgranular zone (SGZ) of the hippocampal DG proliferate and differentiate into mature neurons, oligodendrocytes, and astrocytes [5, 6]. While research has focused on understanding how differentiated neurons contribute to anxiety, astrocytes also play an important role in modulating anxiety-like behaviors in mice [4]. Hence, it is crucial to extensively explore hippocampal neurogenesis concerning the influence of neuromodulation on anxiety-like behavior.

Light signals regulate various physiological and behavioral processes throughout life. As a nonpharmacological tool, light is invaluable for promoting neurogenesis. In our previous study, we found that visible blue light promotes NSC differentiation via OPN4 (melanopsin/Opsin 4)/transient receptor potential channel 6 (TRPC6) modulators [7]. It has been recently reported that NIR light can enhance learning and memory in both humans and animal models [8, 9]. NIR light has also been associated with reducing neuroinflammation and preventing cognitive decline associated with neurodegenerative states [10]. These findings indicate that NIR radiation is a potential therapeutic strategy for the treatment of anxiety. However, information on the response of NSCs to NIR stimulation and neurogenesis in the modulation of anxiety-like behaviors is limited.

Several studies have demonstrated that exposing mouse models with Alzheimer's disease to flickering blue light stimulation (40 Hz) affects their cognitive functions [11, 12].This observation is attributed to the reduction of accumulated amyloid-ß (Aß) protein levels and the improvement of microglial function. While recent studies have questioned this mechanism, the synchronization of gamma-band (30–100 Hz) oscillations results in significant behavioral improvements in cognitive functions [13]. Gamma band illumination may carry different spatial frequency information, which can stimulate distinct oscillations in the brain. When considering these findings alongside our previous results, it is evident that the mechanism underlying this observation is significantly associated with gamma band illumination. Despite the vast amount of information regarding the effect of visible light, there is a significant gap in knowledge regarding the response of stem cells to flickering NIR stimulation, particularly in anxiety-like behaviors.

We have previously reported that NSCs express the *Opn4* gene, making them responsive to blue light-based stimulation [7]. OPN4 was first characterized as a non-visual opsin in intrinsically photosensitive retinal ganglion cells, forming a pigment that is maximally sensitive to 460–470 nm blue light [14, 15]. In the present study, we hypothesized that OPN4 serves as a key photoreceptor response to 940 nm NIR irradiation by utilizing second harmonic generation (SHG) for non-absorptive frequency doubling of excitation light [16]. Specifically, we hypothesized that NSCs respond to 940 nm NIR using OPN4 coupled with TRPC6. In this study, we investigated the effects of gamma band NIR (40 Hz) on neurogenesis in the hippocampus, including increased glial activation and anxiolytic effects. Our findings can be used to develop novel and preventative treatments for people with anxiety.

Materials and methods

Animals

All animal studies were approved by the Animal Care and Use Committee of the Shandong University School of Basic Medical Sciences (ECSBMSSDU2023-2-10), and the animal experiments have been reported in accordance with the ARRIVE guidelines.

The animals were weighed and assessed for neurological manifestations prior to surgery. Before surgery, the mice were anesthetized using the universal small animal anesthesia machine (RWD Life Science Co. Ltd, China). General anesthesia was induced by placing the mice in a transparent anesthetic chamber filled with 3–5% isoflurane. The anesthesia was maintained during surgery with 1–2% isoflurane applied to the nostrils of the mice using anesthesia masks for small animals. Mice were checked for the absence of the tail-pinch reflex as a sign of sufficient anesthesia. The mice were then immobilized in a stereotaxic frame, and erythromycin eye ointment was applied to prevent eye drying. The skin wound around the surgical area was closed with dental acrylic. After surgery was complete, mice were allowed to recover from anesthesia on a heating pad.

Chronic restraint stress (CRS) and anxiety-like behavioral studies (elevated plus maze EPM and open field test OFT)

C57BL/6 male mice (8 weeks old) were divided into three groups: (1) control ($n=6$), (2) CRS ($n=6$), and (3) CRS under NIR exposure ($n=6$). CRS mice were placed in a plastic cylinder with access to air and restrained for 2 hours (20:00–22:00) each day for 28 consecutive days. The size of the cylinder was similar to that of the animal, making it almost impossible for the animal to move

within it. The control and CRS groups were treated in the same manner for the same amount of time except that the device was removed. The CRS mice were further divided into two groups that received either optical fiber or optical fiber with NIR illumination (940 nm, 40 Hz, ~75 mW/cm^2, 45 min daily for 7 consecutive days).

Behavioral analysis was performed as previously described [17]. In EPM, the elevated plus maze consisted of four elevated arms (two 35×6×15 cm closed arms, and two 35×6 cm open arms), which radiated from a central platform (6×6 cm) to form a plus shape. The apparatus was arranged 60 cm above the ground. Each mouse was placed into the center platform facing an open arm and was allowed to free explore for 5 min. Recording the time spent in open arms with TopScan (Clever Sys Inc, VA, USA) to measure anxiety-like behaviors. In OFT, each mouse was placed in a lighting open field box made of PVC (40×40×40 cm), and was allowed to free explore for 10 min. Using TopScan (Clever Sys Inc, VA, USA) to record the total time spent in the center zone, accessing for anxiety-like behavior.

Immunofluorescence and immunoblotting

Antibodies against the following proteins were purchased: anti-GFAP (ab68428, monoclonal antibody produced in rabbits), anti-S100 (ab868, polyclonal antibody produced in rabbits), anti-PCNA (ab29, monoclonal antibody produced in mice), anti-NeuN (ab177487, monoclonal antibody produced in rabbits), anti-Tuj1(ab14545, monoclonal antibody produced in mice) and anti-OPN4 (ab19383, polyclonal antibody produced in rabbits) purchased from Abcam, USA, anti-NeuN (243078, monoclonal antibody produced in rabbits) purchased from Cell Signaling Technology, MA, USA, anti-PSD95 (CY5407, polyclonal antibody produced in rabbits) and anti-GAPDH (AB0037, monoclonal antibody produced in rabbits) purchased from Abways Technology, Shanghai, China.

At the end of experiments, mice were anesthetized with 1% sodium pentobarbital (50 mg/kg), administered intraperitoneally. The brain tissue was collected after euthanasia. The mouse brains were first fixed in 4% paraformaldehyde in PBS overnight at room temperature at 4ºC and were sectioned at paraffin-embedding samples (Thermo Scientific Sliding Microm, USA). Immunofluorescence and immunoblotting assays were performed as previously described [7]. Fluorescence images were acquired on NEXCOPE-NE910FL microscope.To obtain the mean intensity of immunofluorescence, we used Image-J software to circle the hippocampal DG area to measure the total intensity of immunofluorescence on the area. For each fluorescent image, background was removed through thresholding (value of 40–255 for GFAP and S100, value of 50–255 for PCNA, and value of 110–255 for MAP2).

NIR light stimulation of endogenous NSCs within the DG

We randomly divided 8-week-old C57BL/6 mice to assess NIR stimulation effects on adult neurogenesis within the DG (AP: −1.90 mm, ML: +/−1.25 mm, DV: −2.00 mm). An optical fiber tip emitting light of 940 nm (200 μm in diameter) was positioned within the designated zone. In order to reduce variance in experimental animal, we designed to use the left and right side of one mouse's hippocampus as the control group and experimental group, respectively. NIR light pulses of 30 mW/cm^2 and 90 min duration at 40 Hz (12.5 ms pulses) were delivered onto the optic fiber to photostimulate endogenous NSCs.

To measure proliferation in C57BL/6 mice post 90-min NIR exposure, adult mice were given four intraperitoneal injections of 50 mg/kg EdU (10 mg/ml with 0.9% NaCl) 8 h before illumination. Following a 72 h interval, mice were transcardially perfused and the brain tissues were collected and sliced into 10 μm sections for immunofluorescence assays. We used Image J software to circle the hippocampal DG area to measure the total number of positive cells.

In vivo calcium recording of NIR-stimulated mice with fiber photometry

The rAAV-GfaABC1D-Cyto-GCaMP6f virus (3.12×10^{12} vp/ml, BC-0378, Braincase, Shenzhen, China) was injected into the DG of male C57BL/6 mice. After 10 days of virus expression, we performed an in vivo photostimulation experiment using optical fiber illumination (40 Hz NIR light with an irradiation time of 45 min daily for seven consecutive days), and GCaMP6f fluorescence from the hippocampus was recorded to obtain baseline calcium activity data. To record fluorescence signals, the fiber photometry system (Tinker Tech Biotech, Nanjing, China) used two continuous sinusoidally modulated LEDs at 470 nm and 410 nm as light sources to excite GCaMP6f and an isosbestic autofluorescence signal, respectively. When GCaMP6f was excited at 470 nm, the emitted fluorescence intensity was Ca^{2+} sensitive; however, when excited at 410 nm, the emission was largely Ca^{2+}-insensitive, which was used as a control.

Stereotactic injection

The shRNA was used to silence the expression of *Opn4*. Custom-made AAV vectors carrying shRNA targeting mouse *Opn4* (shRNA-*Opn4*) and control AAV-CMV (shRNA- control) were purchased from GeneChem Biotechnology Co., Ltd. (Shanghai, China). Animals were randomly divided into shRNA-Control and shRNA-*Opn4* groups and code labeled by an independent researcher. After a one week acclimatization period, the mice were

fixed in the stereotaxic apparatus (RWD instruments) and anesthetized with isoflurane (3.0% for induction and 1.5% for maintenance). Using an automatic microinjection system (RWD Instruments), shRNA-control and shRNA-*Opn4* were bilaterally injected into the hippocampus DG region according to the following coordinates: AP = −1.9; ML = ±1.25; DV = −2.0. Injections were performed at a speed of 0.1 μL/min using a Hamilton needle (1 μL, 7.5×10^{12} viral particles per mL).

Cell culture

NSC isolation and culture were performed as previously described [7]. The cells were maintained in a growth medium (Gibco21103049, Thermo Fisher, MA, USA) containing NeuroCult™ SM1 Without Vitamin A (STEMCELL Technologies, BC, USA), 20 ng/ml bFGF and EGF (Thermo Fisher, MA, USA) at 37 °C with 5% CO_2, exposed to 940 nm NIR light (Yuanming Laserver, Ningbo, China). The treatment group received 40 Hz NIR exposure at 15 mW/cm^2, 90 min daily for five consecutive days.

The number of neurospheres indicates the proliferation potential of NSCs. The cells were plated at 10,000 cells per well in 24-well plates. After 5 days, the number of neurospheres (>50 μm in size) was counted. Four wells were used for quantifying the number of neurospheres. The EdU incorporation for cell proliferation and immunofluorescence assays were performed in NSC cultures, as previously described [7].

For NSC differentiation, the neurospheres were dissociated into single cells. Next, the cells were plated at 80,000 cells per well in 24-well plates with coverslips in differentiation medium (Neurobasal medium and SM1 supplement, Thermo Fisher) containing 10% FBS (Thermo Fisher) without bFGF and EGF. Both the 24-well plates and coverslip were coated with Matrigel(Corning BD Biocoat, USA) before use. Cells immunostained 5 days after the induction and were fixed using 4% paraformaldehyde in PBS. To investigate the role of the photoreceptor, we used Opsinamide AA92593 (SML0865, Sigma-Aldrich, MO, USA), a selective competitive antagonist of the photoreceptor OPN4 (melanopsin), based on a previous study [18]. Neural cells were divided into three groups: (1) control group; (2) NIR-stimulated group; (3) NIR-stimulated group in the presence of AA92593 (1.5 μM).

Statistical analysis

The data are presented as means ± SEM. Data from the two groups were evaluated statistically using a two-tailed unpaired *t* test for significant differences. Values of $p<0.05$ were considered to indicate statistical significance ($^{*}p<0.05$, $^{**}p<0.01$, and $^{***}p<0.001$). GraphPad Prism 5.0 (GraphPad Software Inc., San Diego, CA, USA) was used for all statistical analyses.

Results

NIR illumination reduces anxiety-like behaviors in CRS mice

First, we assessed whether NIR illumination of the hippocampus reduced anxiety-like behaviors in the EPM and OFT. As shown in Fig. 1A, CRS-induced anxiety model mice were generated by 28 consecutive days of restraint stress, following which they were divided into two groups that received either optical fiber or optical fiber with NIR illumination (940 nm, ~75 mW/cm^2, 40 Hz). To verify the anxiety-like behavior of CRS mice, we used immunoblotting experiments to observe the change of PSD95, TUJ1and GFAP expression (Supplementary Fig.S1A). In the EPM (Fig. 1B), NIR-treated mice exhibited a significant increase in exploration time in the open arm (Fig. 1C) and the number of entries (Fig. 1D) compared with CRS mice with anxiety-like behavior. In the OFT (Fig. 1E), NIR-treated mice traveled longer in the center than CRS mice. NIR-treated mice showed a significant increase in exploration based on time in the center (Fig. 1F) and total distance traveled (Fig. 1G). Additionally, we used immunoblotting experiments to verify the change of PSD95, TUJ1and GFAP expression upon NIR exposure (Supplementary Fig. S1B). Overall, these results suggest that NIR light has the potential to modulate anxiety-like behavior.

NIR compensates for the depression-related reduction in hippocampal astrocytes

Accumulating evidence suggests that neural precursor proliferation and neurogenesis decrease significantly during depression, concomitant with a decline in the associated OFT and EMP behavioral functions [19]. Proliferating cell nuclear antigen (PCNA) is abundantly expressed in proliferating cells, therefore we first measured PCNA expression in the hippocampus of mice receiving CRS + NIR treatment using immunofluorescence assays. As shown in Fig. 2A and B, our results revealed that the NIR-treated group had over 1.4-fold higher PCNA expression in the hippocampus compared with the CRS-induced group. However, quiescent NSCs are characterized by the lack of expression of proliferation markers and will be referred to proliferation-competent cell state. Furthermore, we measured GFAP expression in the hippocampus of mice receiving CRS + NIR treatment. Astrocytes (GFAP immunofluorescence positive) provide metabolic support to their partner neurons and critical during neurogenesis.As shown in Fig. 2C and D, our results revealed that the NIR-treated group had over 1.7-fold higher GFAP expression compared with the CRS-induced group. In line with this result, we found

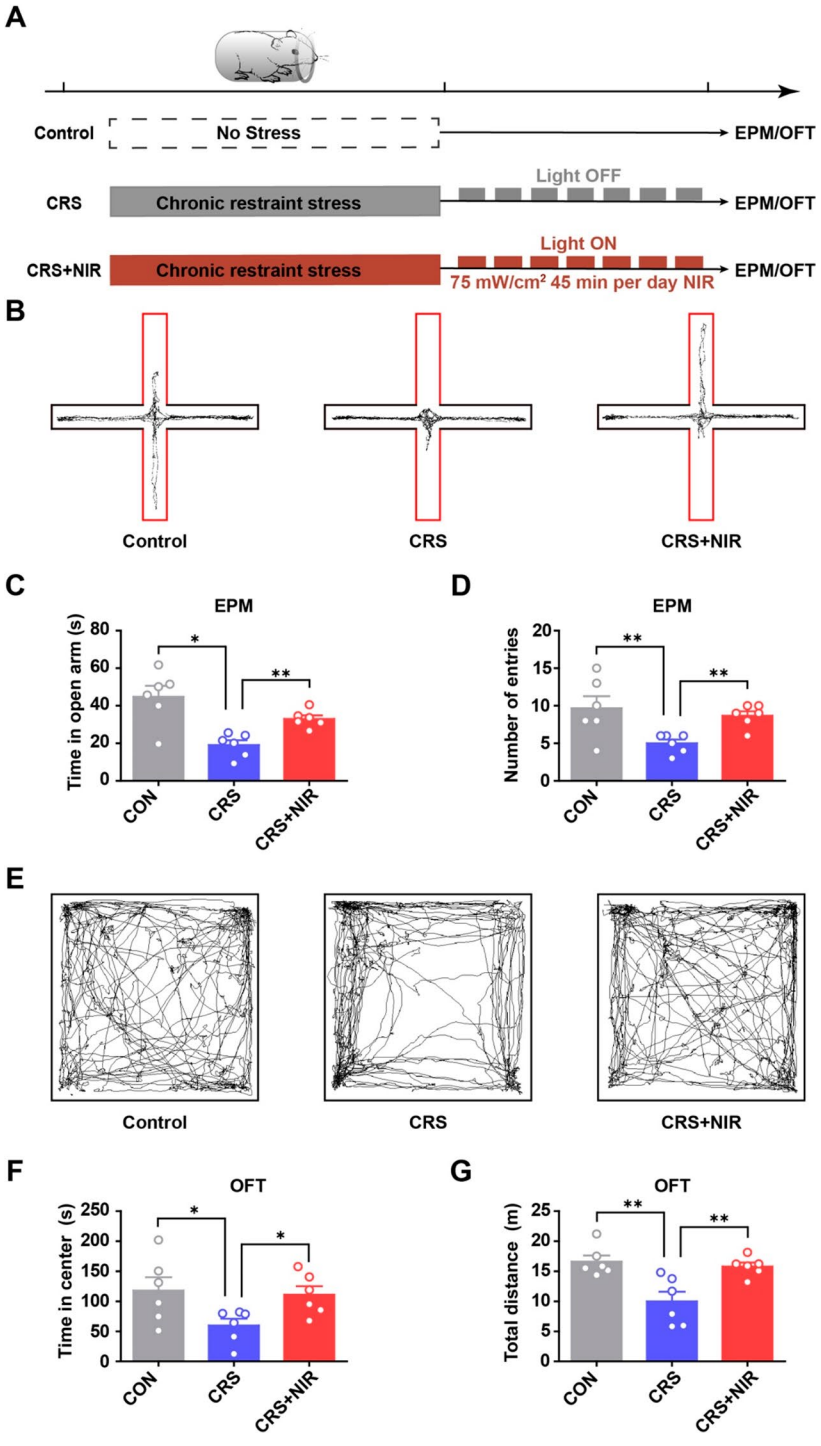

Fig. 1 Behavioral test of CRS mice under NIR illumination. **(A)** Experimental scheme outlining the indicated treatments and behavioral experiments conducted. **(B-D)** Results of EPM (CON: $n=6$; CRS: $n=6$; CRS + NIR: $n=6$. Values represent mean ± SEM, $^{*}p<0.05$ and $^{**}p<0.01$. **(B)** Representative locomotion trajectories of mice in the EPM. **(C)** Time spent by mice in the open arm of EPM. **(D)** Number of mice entering the open-arm in the EPM. **(E-G)** Results of OFT (CON: $n=6$; CRS: $n=6$; CRS + NIR: $n=6$). Values represent mean ± SEM, $^{*}p<0.05$ and $^{**}p<0.01$. **(E)** Representative locomotion trajectories of mice in the OFT. **(F)** Time spent by mice in the central area of OFT. **(G)** Distance travelled by mice in the OFT

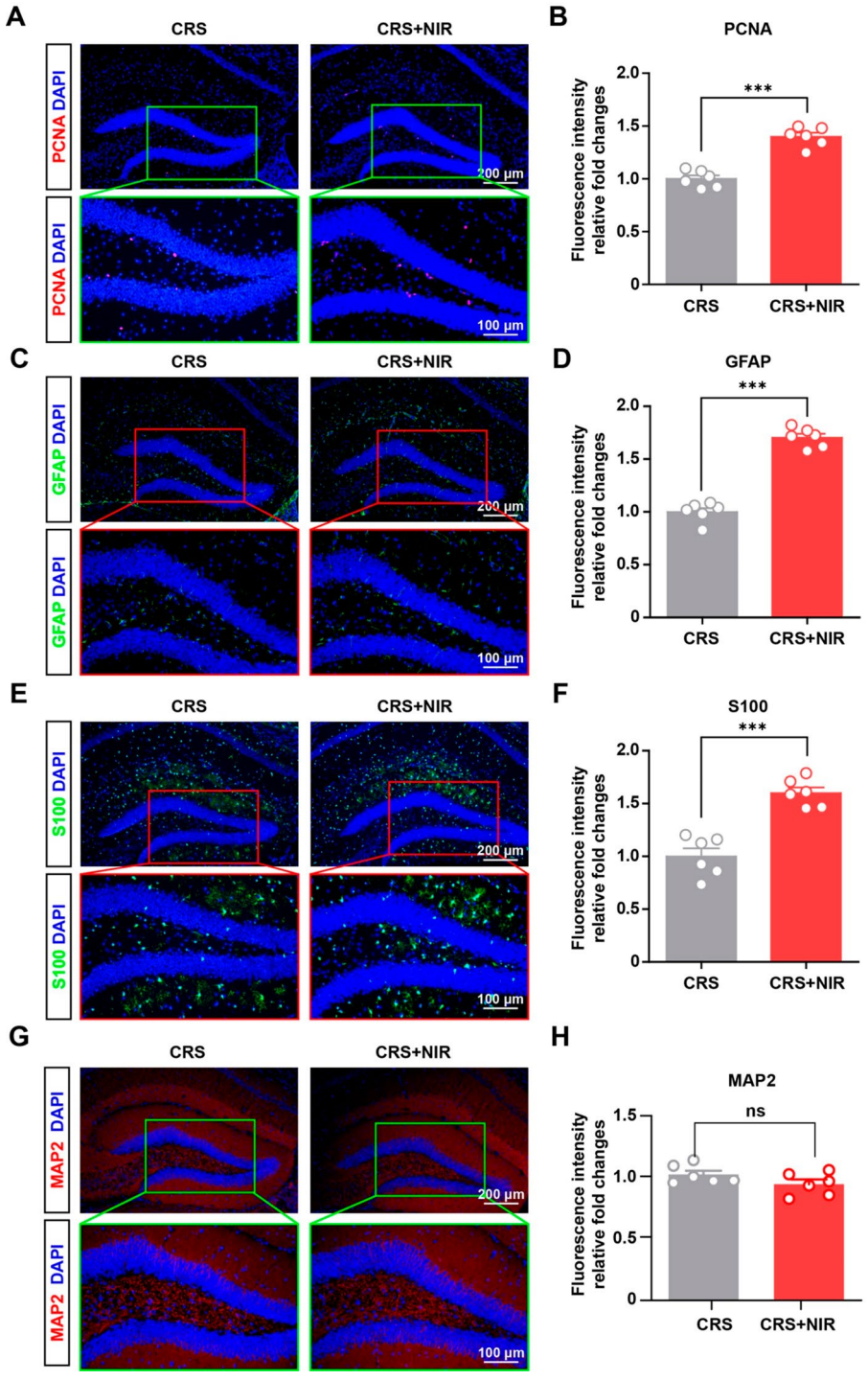

Fig. 2 Glial expression in the hippocampus of CRS mice after NIR treatment. **(A)** Representative image of immunohistochemical staining for PCNA in the non-stimulated and stimulated DG regions of CRS mice. **(B)** Relative intensity value of fluorescence after homogenization (CRS: $n = 3$; CRS + NIR: $n = 3$; two slices per mice). **(C)** Representative images of immunofluorescence staining of GFAP in the non-stimulated and stimulated DG regions of CRS mice. **(D)** Relative intensity value of fluorescence after homogenization (CRS: $n = 3$; CRS + NIR: $n = 3$; two slices per mice). **(E)** Representative image of immunohistochemical staining for S100 in the non-stimulated and stimulated DG regions of CRS mice. **(F)** Relative intensity value of fluorescence after homogenization (CRS: $n = 3$; CRS + NIR: $n = 3$; two slices per mice).Values represent mean ± SEM, $^{***}p < 0.001$. **(G)** Representative image of immunohistochemical staining for MAP2 in the non-stimulated and stimulated SGZ regions of CRS mice. **(H)** Relative intensity value of fluorescence after homogenization (CRS: $n = 3$; CRS + NIR: $n = 3$; two slices per mice).Values represent mean ± SEM, $^{***}p < 0.001$

significantly higher levels of S100 expression under NIR exposure (Fig. 2E and F), which may explain why astrocytes responded to NIR illumination to decrease anxiety-like behaviors. Additionally, the MAP2 immunosignal in the irradiated group was not significantly different from that in the control group (Fig. 2G and H), suggesting the whole neuronal population remained unchanged with the methodology used. A more complete analysis of neurogenesis upon NIR exposure need further exploration. Taken together, these findings indicate that NIR treatment can restore depression-related astrocytic deficits in hippocampal function.

NIR induces NSC proliferation and differentiation in vivo

Our previous studies demonstrated the expression of OPN4-TRPC6 in the SGZ region of the mouse brain, indicating the constitutional expression of photoreceptors in endogenous NSCs [7]. We sought to determine whether NIR irradiation increases neurogenesis in vivo. To investigate this, we used an optical fiber (940 nm, ~30 W/cm^2, 40 Hz) to illuminate the SGZ for 90 min (Fig. 3A). We found that NIR treatment resulted in a greater than 1.6-fold increase in the number of proliferating cells in the DG (Fig. 3B and C).

We determined whether NIR could increase differentiation, in addition to increasing the number of proliferating precursor cells. We confirmed that 40 Hz NIR induced hippocampal astrocyte differentiation compared with 10 Hz and 20 Hz NIR exposure (Supplementary Fig. S2A). As shown in Fig. 3D and E, GFAP immunosignals in the NIR group were significantly higher than those in the control group. In addition, EdU, GFAP and double staining fluorescence triggered with NIR illumination were verified upon 45 min daily for 7 consecutive days exposure (Supplementary Fig. 2B-2E). To detect neuronal differentiation, NeuN (a neuronal marker) immunofluorescence was performed after light stimulation (Fig. 3F). The NeuN immunosignal in the irradiated group was not significantly different from that in the control group (Fig. 3G). Moreover, the influence of NIR irradiation on endogenous NSC differentiation was verified using western blotting. Notably, GFAP protein levels were significantly higher in DG under NIR light exposure (Fig. 3H and I). Overall, these results demonstrate that NIR irradiation enhance NSCs proliferation in vivo and significantly stimulate astrocyte differentiation in the mouse brain.

NIR stimulates hippocampal astrocytes by increasing calcium activity

To verify that NIR irradiation promotes astrocyte differentiation in the hippocampus, the hippocampal astrocytic Ca^{2+} activity was monitored in vivo using fluorescence photometry (Fig. 4A). As shown in Fig. 4B, the GCaMP6 virus (rAAV-GfaABC1D-Cyto-GCaMP6f) was injected into the hippocampus of C57BL/6 mice, which expressed cytosolic GCaMP6f in astrocytes located in the hippocampus. Fiber photometry experiments demonstrated increased baseline calcium signals in the hippocampal astrocytes of one NIR-treated mouse compared with a mock control (Fig. 4C and D). Averaging the baseline calcium activity over the population of animals showed that the NIR-treated group exhibited over 1.4-fold higher in calcium peaks and 1.7-fold higher areas under the curve individually (Fig. 4E and F). Furthermore, we measured the astrocytic Ca^{2+} activity in the hippocampus of mice receiving CRS+NIR treatment (Fig. 4G and H). As shown in Fig. 4I and J, our results revealed that the NIR-treated CRS mice had over 2.3-fold higher calcium peaks and 2.2-fold higher areas under the curve individually. We found that the NIR irradiation exhibited greater astrocytic calcium activity both in control and CRS-induced mice. Collectively, these results confirm that NIR induces an increase in intracellular calcium levels in hippocampal astrocytes.

NIR light induces NSC proliferation and differentiation via OPN4

Finally, we used in vitro NSCs (Supplementary Fig. 2F) and verified the response of NSCs to an NIR light via OPN4. We infused shRNA-*Opn4* into the SGZ mediating *Opn4* knockdown (Fig. 5A). Under NIR exposure, the expression of *Opn4* in the SGZ area was remarkably reduced after shRNA-*Opn4* virus transduction compared with the control vector (shRNA-control) (Fig. 5B). Under NIR exposure, GFAP immunofluorescence levels in the hippocampus were significantly decreased by shRNA-*Opn4* intervention, validating OPN4 mediating the induction (Fig. 5C and D).

Figure 5E shows a significant increase in neurosphere generation following treatment with NIR light in vitro. NIR light-sensitive proliferation was reversibly inhibited by AA92593, the pharmacological inhibitor of OPN4 (Fig. 5F). As shown in Fig. 5G and H, proliferation was enhanced in the NIR light treated group (21.5±1.5% EdU-positive) compared with the time-matched dark control group (14.7±1.9% EdU-positive), and was also reversibly inhibited by AA92593 (13.1±1.5% EdU-positive). The number of the spheres produced during each passage would be observed to explore NSCs self-renewal in the further study.

The results suggested that NIR light promotes astrocyte differentiation. Since NIR light reportedly increases thermo-temperature, we monitored the temperature of the culture medium under light exposure and in controls under dark conditions. On average, the medium temperature under NIR irradiation was less than 0.1 °C higher than that of the dark control. Collectively, these findings

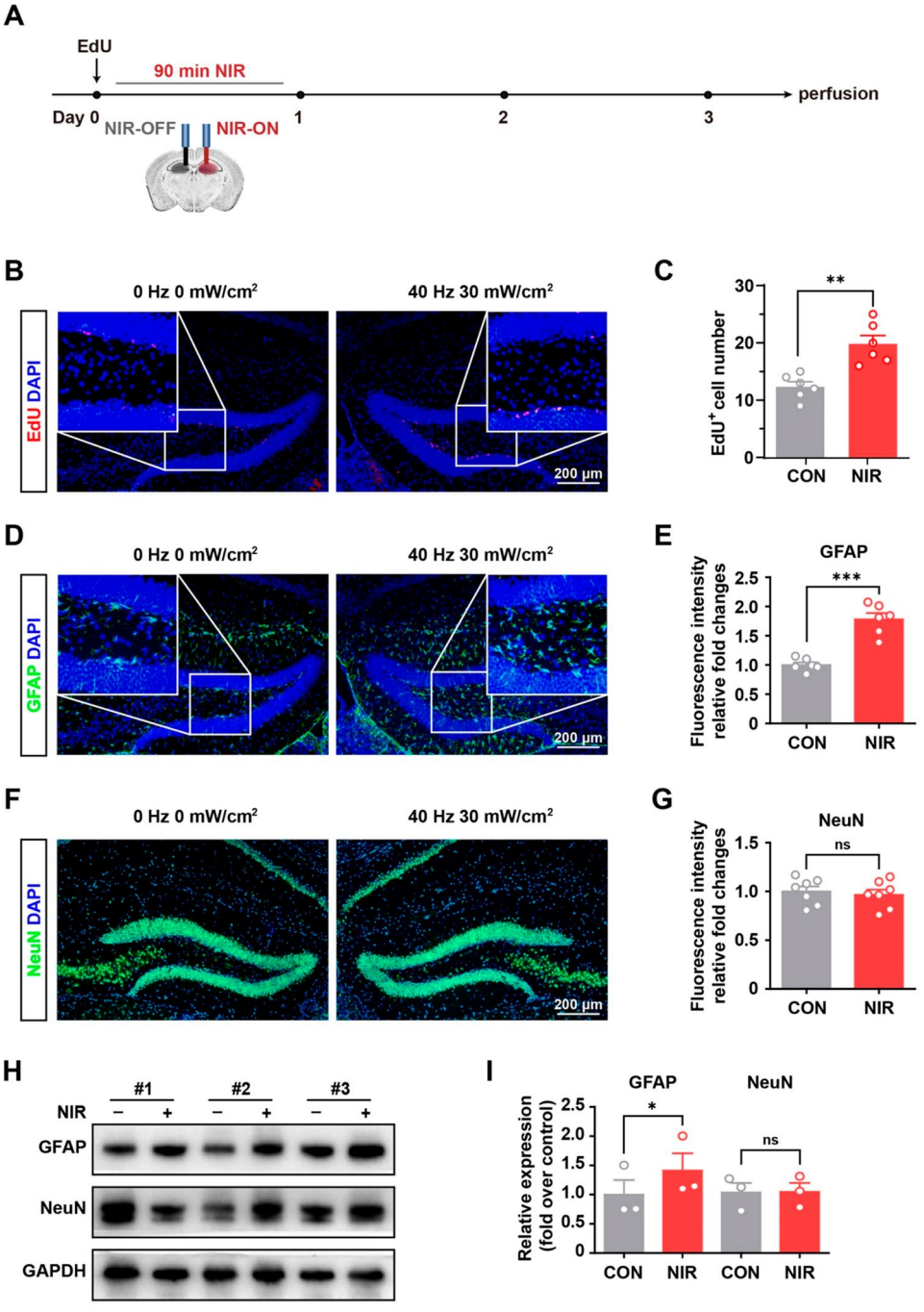

Fig. 3 NIR stimulated hippocampal neurogenesis in vivo by nongenetic stimulation. **(A)** Schematic flowchart of nongenetic NIR stimulation experiment. **(B)** Immunofluorescence staining of EdU incorporation assay of NSCs in DG under NIR exposure. **(C)** Statistical analysis of EdU positive cells using Image-J software ($n=6$ slices/3 mice/group, the left DG with only the optical fiber was used as a control after light stimulation for each animal) **(D)** Representative images of immunofluorescence staining of GFAP in the non-stimulated and stimulated DG regions as described in the experimental procedures. **(E)** Statistical analysis of immunosignals using Image-J software ($n=6$ mice per group, the left DG with only the optical fiber was used as a control after light stimulation for each animal). **(F)** Representative images of immunofluorescence staining of NeuN in the non-stimulated and stimulated DG regions as described in the experimental procedures. **(G)** Statistical analysis of immunosignals using Image-J software ($n=7$ mice per group, the left DG with only the optical fiber was used as a control after light stimulation for each animal).Values are presented as mean ± SEM. Values are presented as mean ± SEM. $^{**}p<0.01$, $^{***}p<0.001$. **(H)** Equivalent amounts (30 μg) of tissue lysates were separated by SDS-PAGE and analyzed by immunoblotting with antibodies specific for the indicated proteins. GAPDH was used as a loading control ($n=3$ mice per group, the left SGZ with only the optical fiber was used as a control after light stimulation for each animal). **(I)** Statistical analysis of immunosignals. Values are presented as mean ± SEM. $^{*}p<0.05$

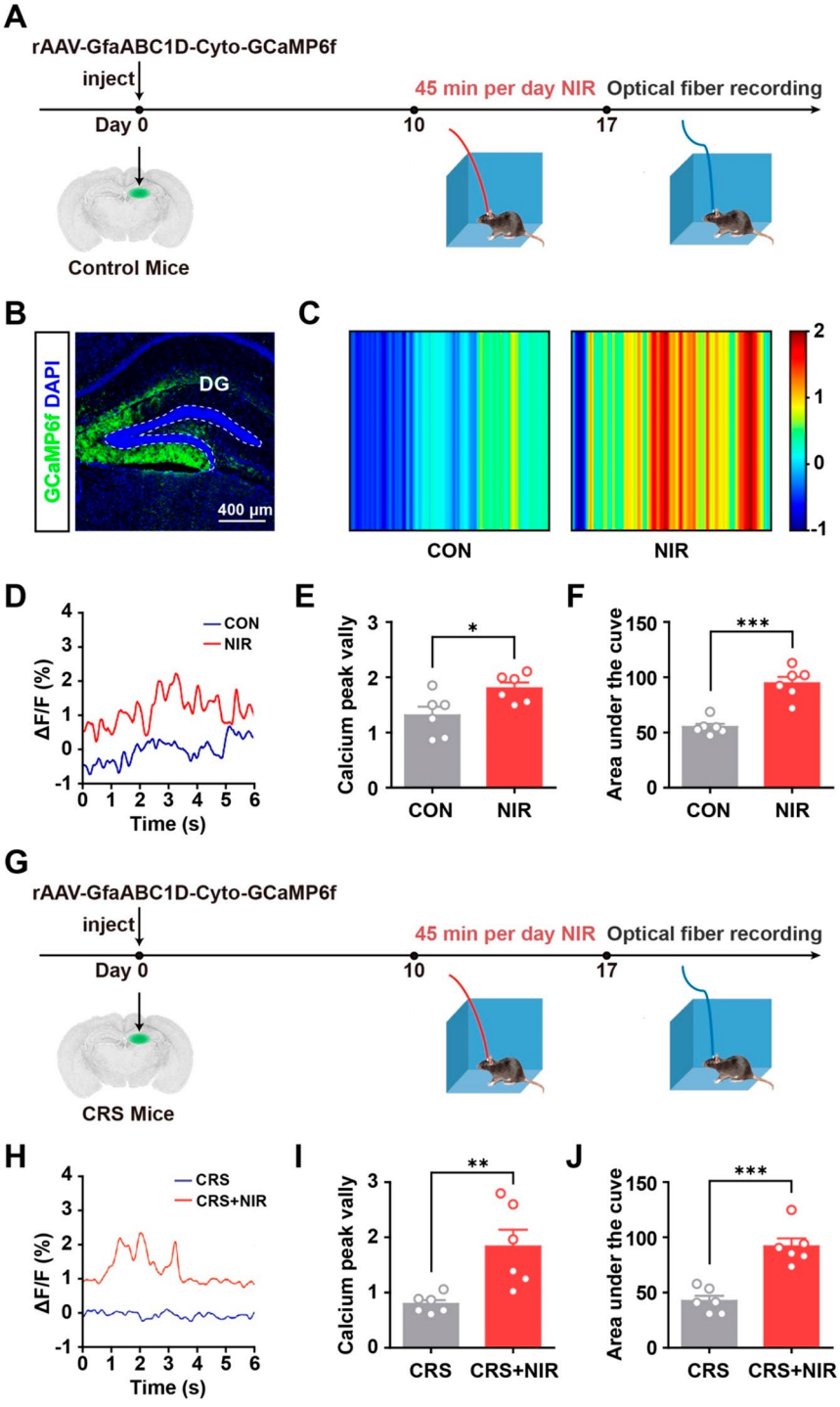

Fig. 4 In vivo calcium recordings in awake mice using optical fiber photometry. **(A)** Experimental protocol for calcium signal recording with optical fiber photometry in C57BL/6 mice. **(B)** Immunofluorescence image showing GCaMP6f expressed astrocytes in the DG. **(C)** Color plot depicting DG Ca^{2+} activity in the non-stimulated and stimulated mice. **(D)** Sample ΔF/F of GCaMP6f signals from the DG in non-stimulated and stimulated mice. **(E)** Bar graphs illustrating the peak valley of calcium signal in non-stimulated and stimulated mice DG regions as described in the experimental procedures ($n = 6$ mice per group). **(F)** Bar graphs showing the integration under the curve of calcium signal in non-stimulated and stimulated mice DG regions as described in the experimental procedures ($n = 6$ mice per group). **(G)** Experimental protocol for calcium signal recording with optical fiber photometry in CRS mice. **(H)** Sample ΔF/F of GCaMP6f signals from the DG in non-stimulated and stimulated CRS mice. **(I)** Bar graphs illustrating the peak valley of calcium signal in non-stimulated and stimulated CRS mice DG regions as described in the experimental procedures ($n = 6$ mice per group). **(F)** Bar graphs showing the integration under the curve of calcium signal in non-stimulated and stimulated CRS mice DG regions as described in the experimental procedures ($n = 6$ mice per group). Values are presented as mean ± SEM, $^{*}p < 0.05$, $^{**}p < 0.01$, $^{***}p < 0.001$

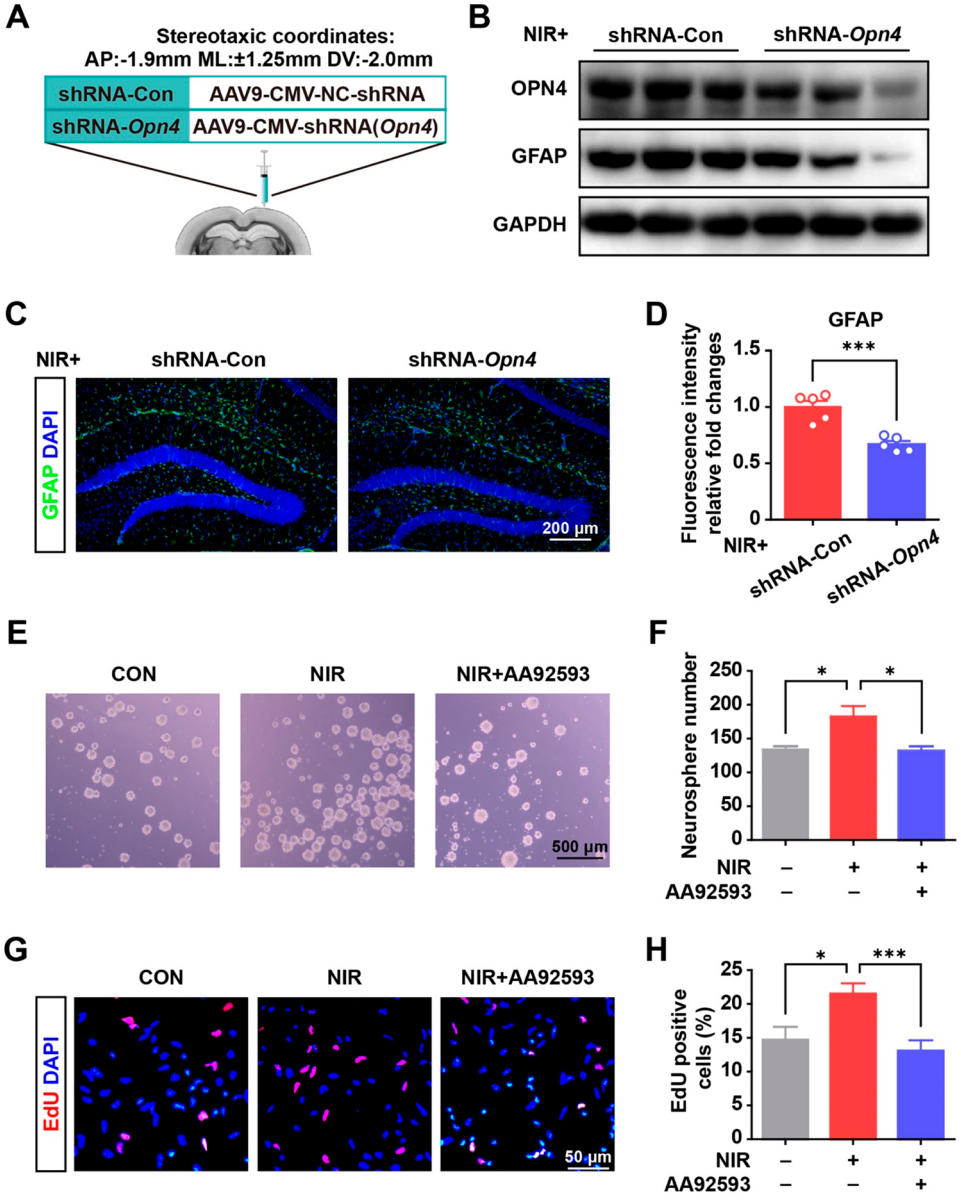

Fig. 5 NIR irradiation promoted NSC proliferation and astrocyte differentiation **(A)** Scheme of the experimental design. **(B)** shRNA-*Opn4* injection down-regulated OPN4 and GFAP expression in the hippocampus of mice with NIR irradiation. **(C)** Immunofluorescence staining for GFAP in the control and shRNA-*Opn4* group with NIR irradiation. **(D)** Quantitative data from immunofluorescence staining (5 slices from 3 mice for each group). Values are presented as mean ± SEM, ***$p < 0.001$. **(E)** Representative micrographs of NSC sphere formation after NIR irradiation and Opn4 inhibitor (AA92593) treatment. **(F)** Quantitative data from NSC sphere counts with the indicated treatment. The results from four repeat wells of a 24-well plate. Values are given as mean ± SEM. *$p < 0.05$. **(G)** Photographs of the EdU incorporation assay of NSCs under NIR exposure. **(H)** Quantitative data from NSC proliferation under illumination across 12–13 randomly selected view fields of the tested samples using ImageJ software. Values are given as mean ± SEM. *$P < 0.05$, and ***$P < 0.001$

verified that NIR light effectively triggers NSC proliferation and glial differentiation via the OPN4 photoreceptor.

Discussion

Stress profoundly impacts neurogenesis, leading to rapid and prolonged decreases in cell proliferation in the adult hippocampus [20]. Notably, alternations in astrocytes have been observed in the brains of individuals with anxiety or depression as well as in animal models [4]. The studies of postmortem human brain showed alteration of astrocytic morphology and volume in mood disorder [21]. In addition, astrocytes are implicated in anxiety-like behavior in the rat PTSD animal model, and astrocytes activation in the central amygdala reduces anxiety-like behaviors in rodents [22]. Astrocytes interacts with neurons and can modulate synaptic plasticity,

and disruptions in these interactions may be involved in anxiety pathogenesis. Astrocytes release various synaptic transmitters and modulators, such as glutamate, D-serine, ATP/adenosine, GABA, and lactate, via calcium-dependent and -independent signaling pathways [23]. Notably, hippocampal astrocytes express oxytocin receptors, and oxytocin released in amygdala activate astrocyte Ca^{2+} signal through oxytocin receptor and mediate its anxiolytic effects [22]. Exposure to 40 Hz flickering light has been demonstrated to stimulate learning and memory abilities [11]. Furthermore, multiple gamma oscillations play distinct roles in cognitive functions, especially learning [13]. However, the underlying mechanisms driving these changes remain unclear. In this study, we found that exposure to 40 Hz NIR induced hippocampal astrocyte differentiation and calcium-dependent activity. Stimulation of astrocytic calcium signaling can improve anxiety-like behaviors triggered by stress [24]. Our findings suggest that NIR irradiation can activate hippocampal NSCs, resulting in increased proliferation and astrocyte differentiation. Additionally, our findings illustrate that the mechanism underlying the regulation of flicking light, particularly gamma-band oscillations (30–100 Hz), can regulate deep brain regions.

NIR treatment has been studied over the last 30 years for its role in pain relief, wound healing, and anti-inflammatory effects. Accumulating evidence indicates that NIR radiation is a novel optogenetic treatment for various CNS pathologies [8, 10], offering distinct advantages over other clinical technologies. Unlike the application of visible spectrum light for optogenetics, NIR manipulation allows for focused stimulation and can be used without genetic manipulation. Recent studies show that NIR irradiation enhances proliferation and differentiation of adipose stem cells via TRP channels [25]. Our results suggest that 40 Hz NIR radiation increases hippocampal proliferation and astrocyte differentiation in the endogenous DG. Notably, factors influencing neurogenesis are associated with depression and antidepressant effects. While stress leads to a rapid and prolonged decrease in the rate of cell proliferation in the adult hippocampus, chronic antidepressant treatment upregulates hippocampal neurogenesis [1]. We propose that this finding provides a potential tool for improving anxiety-like behaviors, often linked to impaired calcium signaling in astrocytes [26]. Based on this hypothesis, we found that NIR illumination increased cellular Ca^{2+} levels in hippocampal astrocytes and triggered the proliferation and differentiation of NSCs into astrocytes.

We previously reported that NSCs in these regions constitutionally express photoreceptors sensitive to visible blue light [7]. As the neurogenesis-enhancing effects of NIR have been previously demonstrated, we focused on understanding the mechanism behind this photosensitive modulation. Our results suggest that OPN4 antagonists inhibit NIR-induced proliferation and differentiation. Interestingly, OPN4 was first characterized in intrinsically photosensitive retinal ganglion cells as a non-visual opsin, forming a pigment that is maximally sensitive to 470 nm blue light [14, 15]. SHG was first demonstrated as a nonlinear optical phenomenon by Kleinman in 1962 using an excited doubled-frequency laser to obtain a shorter half-wavelength [16, 27]. Key endogenous proteins organized in ordered arrays, such as collagen, myosin, and tubulin, produce strong SHG across various species, cell types, and tissues [28]. The results of the present study were consistent with our hypothesis as the activation of G_q-coupled OPN4 by NIR irradiation triggered calcium influx into the cytosol via TRPC6 activation.

NIR light has the potential to be used in treating neurological diseases through enhancing differentiation of NSCs. This is important for neural repair and restoration of function in neurological disorders. However, it's important to note that it is still an area of ongoing research and many factors need to be further studied. The effectiveness might vary depending on the specific disease, the stage of the disease and the parameters of NIR illumination.

In this study, we demonstrated that NIR light stimulates hippocampal astrocytes by increasing calcium activity. However, the percentage of active NSCs and newborn astrocytes remains unknown. Furthermore, it would be interesting to further investigate the SHG effects of OPN4 and the resulting nonlinear optical modulation in deep brain activation of animal models. How the photoreceptors and channels work synergistically, what their individual contributions are, and whether they affect the same population of stem cells remain to be determined.

Conclusion

The present study demonstrated that non-genetic NIR modulation can be used to stimulate hippocampal neurogenesis via the OPN4(melanopsin) photoreceptor. Our findings suggest that the intracellular calcium activity—which underlies anxiety-like behaviors—can be partially reversed via 940-nm NIR manipulation in adult mice. Using animal studies, we discovered the mechanism of NIR modulation of adult neurogenesis and its antidepressant effects (Fig. 6). The accessibility and non-invasiveness of NIR make it particularly significant for the treatment of individuals with anxiety who are at risk of developing depression.

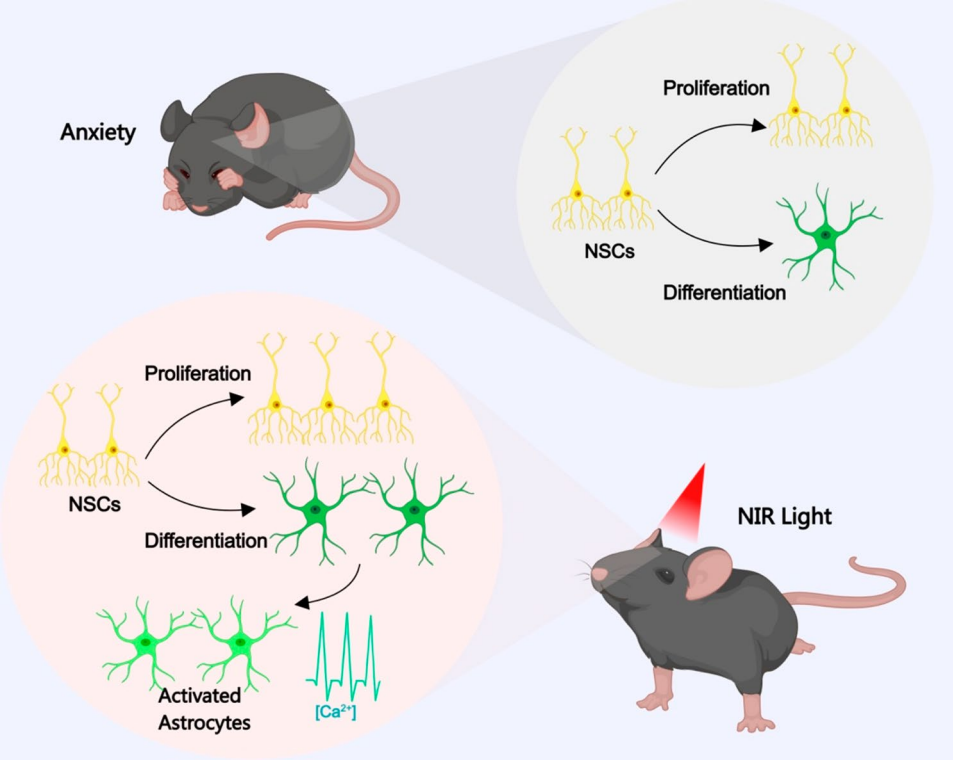

Fig. 6 Schematic representation of our findings showing that NIR light irradiation improved neurogenesis in the hippocampus with anxiolytic effects. See the Discussion section for further details. The image was created using MedPeer.cn

Supplementary Information

The online version contains supplementary material available at https://doi.org/10.1186/s13287-024-04114-3.

Supplementary Material 1: **Supplementary Figure S1: (A)** Representative image (above) and relative intensity value (bottom) of the indicated protein in the control and CRS mice. **(B)** Representative image (above) and relative intensity value (bottom) of the indicated protein in the CRS and CRS+NIR mice. CON: n=3; CRS: n=3; CRS+NIR: n=3.Values represent mean ± SEM, *p < 0.05. **p < 0.01.

Supplementary Material 2: **Supplementary Figure S2: (A)** mRNAs were extracted with 10Hz, 20Hz and 40Hz NIR light illumination and subjected to real-time PCR, respectively. **(B)** Immunofluorescence staining of EdU incorporation (left) and statistical analysis of EdU positive cells (right) under 7 consecutive days exposure (n = 6 slices/3 mice/group). **(C)** Representative images of immunofluorescence staining of GFAP (left) and statistical analysis (right) under 7 consecutive days exposure (n = 6 slices/3 mice/group). **(D)** Double immunofluorescence staining for GFAP/EdU (left) and statistical analysis (right) under 1 day exposure (n = 3 mice per group). (E) Double immunofluorescence staining for GFAP/EdU (left) and statistical analysis (right) under 7 days exposure (n = 3 mice per group). Values represent mean ± SEM, *p < 0.05, *p < 0.01, ***p < 0.001. **(F)** Immunofluorescence staining for Nestin and OPN4 in NSCs. Nuclei were stained using DAPI (blue staining), Nestin (green staining) and OPN4 (red staining) immunostaining.

Supplementary Material 3

Acknowledgements
The authors would like to thank Dr. Qiao Liu (School of Basic Medical Sciences, Shandong University) for illuminating discussions.

Author contributions
XL, QJL, SWL, and DL contributed to the study conception and design. XQ, XCL and YNR contributed to cell culture and studies. XQ and ZLX contributed to the optical modulation system. XQ and XCL contributed to the animal study. ZLX contributed to statistical analyses. YCJ, WJS and JXL contributed to the materials preparation. XL and XQ wrote the manuscript. All authors approved the submitted version and agreed to be accountable for the accuracy and integrity of their contributions.

Funding
This work was supported by the National Natural Science Foundation of China (81873737, 32070586); Natural Science Foundation of Shandong Province-Joint Foundation (ZR2022LZL010).

Data availability
All data generated or analyzed during this study are included in this published article and its additional files. The datasets used during the current study are available from the corresponding author on reasonable request.

Declarations

Ethical approval and consent to participate
The study design and experiments of the project "Near-Infrared Light Induces Neurogenesis and Modulates Anxiety-like Behavior" were approved by the Animal Care and Use Committee of the Shandong University School of Basic Medical Sciences. The approval number is ECSBMSSDU2023-2-10. The date of approval is Feb 10, 2023.

Consent for publication
Not applicable.

Competing interests
The authors declare that they have no competing interests.

Author details
[1]Key Laboratory of Experimental Teratology of the Ministry of Education, Department of Medical Genetics, School of Basic Medical Sciences, Cheeloo College of Medicine, Shandong University, Jinan, Shandong 250012, China
[2]Department of Anatomy and Neurobiology, Research Center for Sectional and Imaging Anatomy, Shandong Provincial Key Laboratory of Mental Disorder, Shandong Key Laboratory of Digital Human and Clinical Anatomy, School of Basic Medical Sciences, Cheeloo College of Medicine, Institute of Brain and Brain-Inspired Science, Shandong University, Shandong University, Jinan, Shandong 250012, China
[3]School of Sports Leisure, Shandong Sport University, Jinan, Shandong 250102, China
[4]Institute of Novel Semiconductors, State Key Laboratory of Crystal Materials, Shandong University, Jinan, Shandong 250100, China
[5]School of Health and Life Sciences, University of Health and Rehabilitation Sciences, Qingdao, Shandong 266071, China

Received: 2 February 2024 / Accepted: 12 December 2024
Published online: 20 December 2024

References

1. Warner-Schmidt JL, Duman RS. Hippocampal neurogenesis: opposing effects of stress and antidepressant treatment. Hippocampus. 2006;16(3):239–49.
2. Palamarchuk IS, Slavich GM, Vaillancourt T, Rajji TK. Stress-related cellular pathophysiology as a crosstalk risk factor for neurocognitive and psychiatric disorders. BMC Neurosci. 2023;24(1):65.
3. Leng L, Zhuang K, Liu Z, Huang C, Gao Y, Chen G, Lin H, Hu Y, Wu D, Shi M, et al. Menin Deficiency leads to depressive-like behaviors in mice by modulating astrocyte-mediated neuroinflammation. Neuron. 2018;100(3):551–e563557.
4. Cho WH, Noh K, Lee BH, Barcelon E, Jun SB, Park HY, Lee SJ. Hippocampal astrocytes modulate anxiety-like behavior. Nat Commun. 2022;13(1):6536.
5. Nie L, Yao D, Chen S, Wang J, Pan C, Wu D, Liu N, Tang Z. Directional induction of neural stem cells, a new therapy for neurodegenerative diseases and ischemic stroke. Cell Death Discov. 2023;9(1):215.
6. Gage FH. Mammalian neural stem cells. Science. 2000;287(5457):1433–8.
7. Wang M, Xu Z, Liu Q, Sun W, Jiang B, Yang K, Li J, Gong Y, Liu Q, Liu D, et al. Nongenetic optical modulation of neural stem cell proliferation and neuronal/glial differentiation. Biomaterials. 2019;225:119539.
8. Chernov M, Roe AW. Infrared neural stimulation: a new stimulation tool for central nervous system applications. Neurophotonics. 2014;1(1):011011.
9. Nizamutdinov D, Qi X, Berman MH, Dougal G, Dayawansa S, Wu E, Yi SS, Stevens AB, Huang JH. Transcranial Near Infrared Light stimulations improve cognition in patients with dementia. Aging Dis. 2021;12(4):954–63.
10. Saieva S, Taglialatela G. Near-infrared light reduces glia activation and modulates neuroinflammation in the brains of diet-induced obese mice. Sci Rep. 2022;12(1):10848.
11. Iaccarino HF, Singer AC, Martorell AJ, Rudenko A, Gao F, Gillingham TZ, Mathys H, Seo J, Kritskiy O, Abdurrob F, et al. Gamma frequency entrainment attenuates amyloid load and modifies microglia. Nature. 2016;540(7632):230–5.
12. Singer AC, Martorell AJ, Douglas JM, Abdurrob F, Attokaren MK, Tipton J, Mathys H, Adaikkan C, Tsai LH. Noninvasive 40-Hz light flicker to recruit microglia and reduce amyloid beta load. Nat Protoc. 2018;13(8):1850–68.
13. Buzsaki G, Moser EI. Memory, navigation and theta rhythm in the hippocampal-entorhinal system. Nat Neurosci. 2013;16(2):130–8.
14. Berson DM, Dunn FA, Takao M. Phototransduction by retinal ganglion cells that set the circadian clock. Science. 2002;295(5557):1070–3.
15. Dacey DM, Liao HW, Peterson BB, Robinson FR, Smith VC, Pokorny J, Yau KW, Gamlin PD. Melanopsin-expressing ganglion cells in primate retina signal colour and irradiance and project to the LGN. Nature. 2005;433(7027):749–54.
16. Campagnola PJ, Millard AC, Terasaki M, Hoppe PE, Malone CJ, Mohler WA. Three-dimensional high-resolution second-harmonic generation imaging of endogenous structural proteins in biological tissues. Biophys J. 2002;82(1 Pt 1):493–508.
17. Gao F, Liu A, Qi X, Wang M, Chen X, Wei S, Gao S, Sun Y, Sun P, Li X et al. Ppp4r3a deficiency leads to depression-like behaviors in mice by modulating the synthesis of synaptic proteins. Dis Model Mech. 2022;15(6).
18. Jones KA, Hatori M, Mure LS, Bramley JR, Artymyshyn R, Hong SP, Marzabadi M, Zhong H, Sprouse J, Zhu Q, et al. Small-molecule antagonists of melanopsin-mediated phototransduction. Nat Chem Biol. 2013;9(10):630–5.
19. Tartt AN, Mariani MB, Hen R, Mann JJ, Boldrini M. Dysregulation of adult hippocampal neuroplasticity in major depression: pathogenesis and therapeutic implications. Mol Psychiatry. 2022;27(6):2689–99.
20. Sha L, Li J, Shen H, Wang Q, Meng P, Zhang X, Deng Y, Zhu W, Xu Q. LHPP-mediated inorganic pyrophosphate hydrolysis-driven lysosomal acidification in astrocytes regulates adult neurogenesis. Cell Rep. 2023;42(8):112975.
21. Muller MB, Lucassen PJ, Yassouridis A, Hoogendijk WJ, Holsboer F, Swaab DF. Neither major depression nor glucocorticoid treatment affects the cellular integrity of the human hippocampus. Eur J Neurosci. 2001;14(10):1603–12.
22. Wahis J, Baudon A, Althammer F, Kerspern D, Goyon S, Hagiwara D, Lefevre A, Barteczko L, Boury-Jamot B, Bellanger B, et al. Astrocytes mediate the effect of oxytocin in the central amygdala on neuronal activity and affective states in rodents. Nat Neurosci. 2021;24(4):529–41.
23. Harada K, Kamiya T, Tsuboi T. Gliotransmitter release from astrocytes: Functional, Developmental, and pathological implications in the brain. Front Neurosci. 2015;9:499.
24. Semyanov A, Henneberger C, Agarwal A. Making sense of astrocytic calcium signals - from acquisition to interpretation. Nat Rev Neurosci. 2020;21(10):551–64.
25. Gholami L, Afshar S, Arkian A, Saeidijam M, Hendi SS, Mahmoudi R, Khorsandi K, Hashemzehi H, Fekrazad R. NIR irradiation of human buccal fat pad adipose stem cells and its effect on TRP ion channels. Lasers Med Sci. 2022;37(9):3681–92.
26. Wang Q, Kong Y, Wu DY, Liu JH, Jie W, You QL, Huang L, Hu J, Chu HD, Gao F, et al. Impaired calcium signaling in astrocytes modulates autism spectrum disorder-like behaviors in mice. Nat Commun. 2021;12(1):3321.
27. Loew LM, Lewis A. Second harmonic imaging of membrane potential. Adv Exp Med Biol. 2015;859:473–92.
28. Vanzi F, Sacconi L, Cicchi R, Pavone FS. Protein conformation and molecular order probed by second-harmonic-generation microscopy. J Biomed Opt. 2012;17(6):060901.

Publisher's note